Supplementary information:

Rationally optimized carrier effective mass and carrier density lead to high average *ZT* value in *n*-type PbSe

Rationally optimized carrier effective mass and carrier density lead to high average *ZT* value in *n*-type PbSe

Yu Xiao,[a,*] Wei Liu,[a] Yang Zhang,[b] Dongyang Wang,[c] Haonan Shi,[c] Sining Wang,[c] Yang Jin,[c] Wanbo Qu,[a] Haijun Wu,[a,*] Xiangdong Ding[a], Jun Sun[a] and Li-Dong Zhao[c]

[a]*State Key Laboratory for Mechanical Behavior of Materials, Xi'an Jiaotong University, Xi'an 710049, China. Email: xiao_yu@xjtu.edu.cn; wuhaijunnavy@xjtu.edu.cn*
[b]*Instrumental Analysis Center of Xi'an Jiaotong University, Xi'an Jiaotong University, Xi'an 710049, China*
[c]*School of Materials Science and Engineering, Beihang University, Beijing 100191, China*

Experimental details

Material synthesis: Raw materials, Pb bulk (99.999%, Aladdin element, China), Se chunk (99.99%, Aladdin element, China), Sb bulk (99.999%, Aladdin element, China), Sn bulk (99.99%, Aladdin element, China), and Ag line (99.99%, Aladdin element, China) were loaded into silica tubes with nominal compositions, flame-sealed at a residual pressure below ~ 10^{-4} Torr, slowly heated to 1323 K in 24 h and maintained at this temperature for 10 h. The furnace was shut down and cooled to room temperature. The obtained ingots were ground into powders and sintered by spark plasma sintering (SPS-211Lx) at 873 K for 12 min under an axial compressive stress of 50 MPa, resulting in highly densified disk-shaped samples.

Structural characterization: The powder X-ray diffraction (PXRD) patterns were obtained with Cu Kα (λ=1.5418 Å) radiation in a reflection geometry on a diffractometer operating at 40 KV and 20 mA and equipped with a position-sensitive detector. The calculation of lattice parameter was performed on the PXRD data with software package Materials Analysis using Diffraction (MAUD). (Scanning) transmission electron microscopy (TEM and STEM) studies were conducted using a JEOL JEM-F200 atomic resolution analytical electron microscope installed in the Instrumental Analysis Center of Xi'an Jiaotong University equipped with a cold field-emission gun. The specimens were prepared by conventional standard methods, that is, cutting, grinding, dimpling, polishing and Ar-ion milling with a liquid nitrogen cooling stage (Fischione M1051 TEM Mill).

Hall measurements: Hall coefficients (R_H) were measured under a reversible magnetic field (0.9 T) by the Van der Pauw method using a Hall measurement system (Lake Shore 8400 Series, Model 8404, USA) from 300 K to 723 K. Carrier density (n_H) was obtained by $n_H = 1/(e \bullet R_H)$, and carrier mobility (μ_H) was calculated using the relationship $\mu_H = \sigma \bullet R_H$ with σ being the measured electrical conductivity.

Band gap measurements: Refined powder was used to measure the optical band gap by Infrared Diffuse Reflection method with a Fourier Transform Infrared Spectrometer (IRAffinity-1S). The spectra was collected in the mid-IR (5000~450

cm^{-1}) and the reflectance to absorption data was converted to estimate the band gap using Kubelka-Munk equation: $\alpha/S = (1-R^2)/(2R)$, where R, S and α are the reflectance, scattering amd absorption coefficients, repectively.

Thermoelectric transport properties: The obtained highly-densified spark plasma sintering (SPS) processed pellets were cut into bars with dimensions around ~ 12 × ~ 3 × ~ 3 mm^3 for simultaneous measurement of the Seebeck coefficient and electrical conductivity using Cryoall CTA instrument under a low-pressure helium atmosphere from 300 to 873 K. The uncertainty of the Seebeck coefficient and electrical conductivity measurement was 5%. The SPS pellets were cut and polished into a disk-like shape with sizes of ~ 6 mm diameter and ~ 2 mm thickness for thermal diffusivity (D) measurements. The samples were coated with a thin layer of graphite to minimize errors from the emissivity method in Netzsch LFA457. The sample density (ρ) was determined using the dimensions and mass of the samples. The specific heat capacity (C_p) was estimated with the Debye model. The thermal diffusivity data was analyzed using a Cowan model with pulse correction. The uncertainty of the thermal conductivity was estimated to be within 8%, considering all the uncertainties from D, ρ and C_p. The combined uncertainty for all measurements involved in the calculation of ZT was less than 20%.

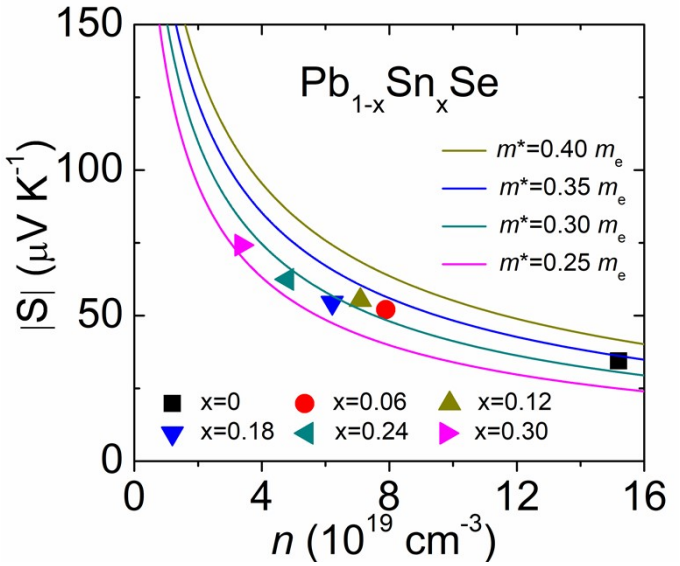

Figure S1. Pisarenko relationship in n-type PbSe with carrier effective mass m_*=0.25, 0.30, 0.35, 0.40 m_e

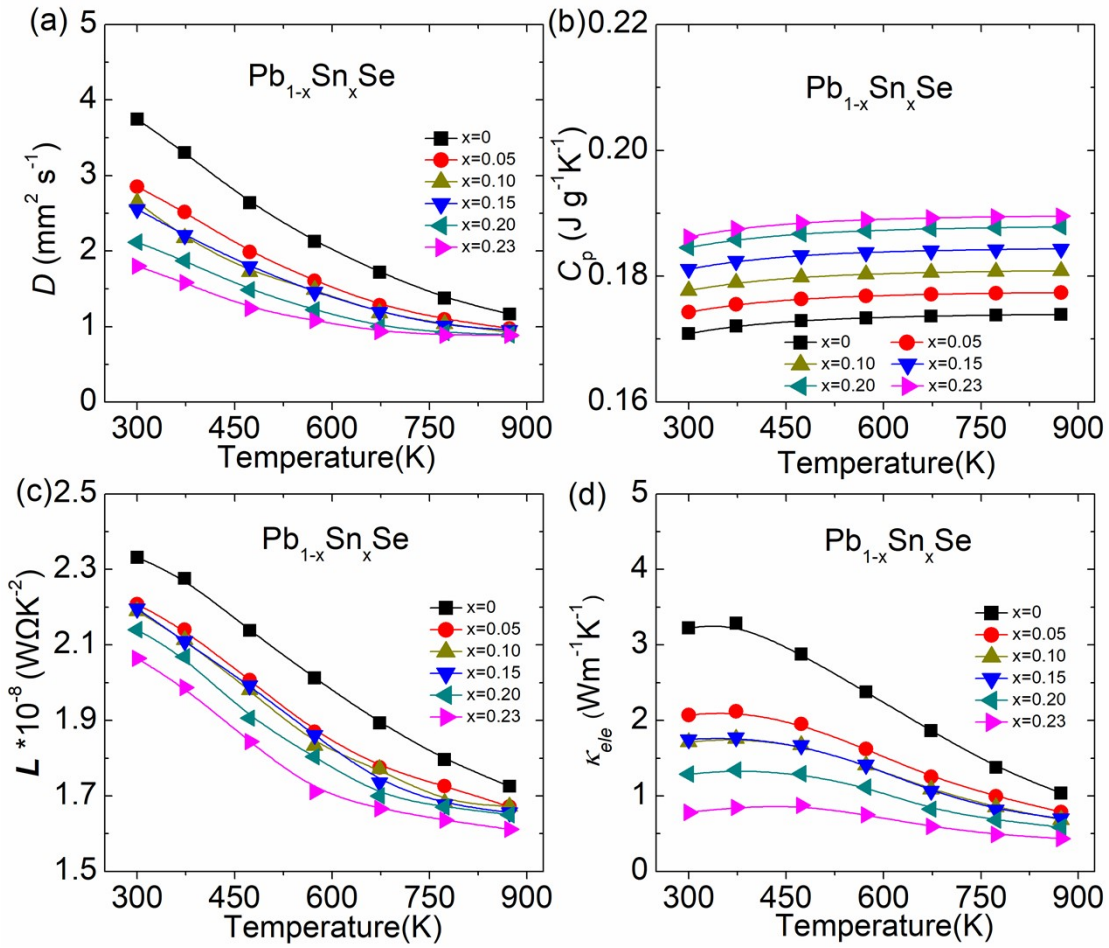

Figure S2. Thermal transport properties of $Pb_{1-x}Sn_xSe$ (x=0-0.23): (a) thermal diffusivity; (b) heat capacity; (c) Lorenz number; and (d) electronic thermal conductivity

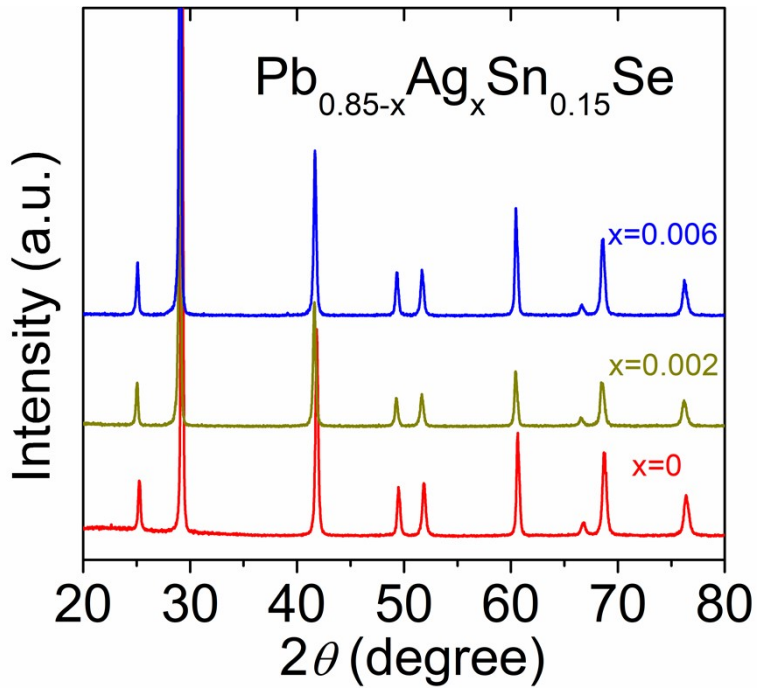

Figure S3. PXRD patterns of $Pb_{0.85}Sn_{0.15}Se$-based samples with Ag doping

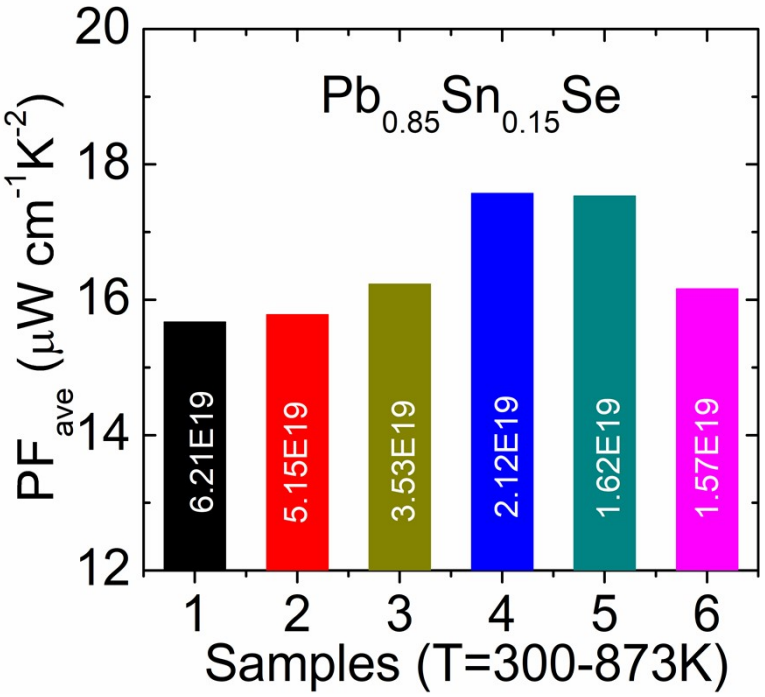

Figure S4. Average power factor of $Pb_{0.85}Sn_{0.15}Se$-based samples at 300-873 K

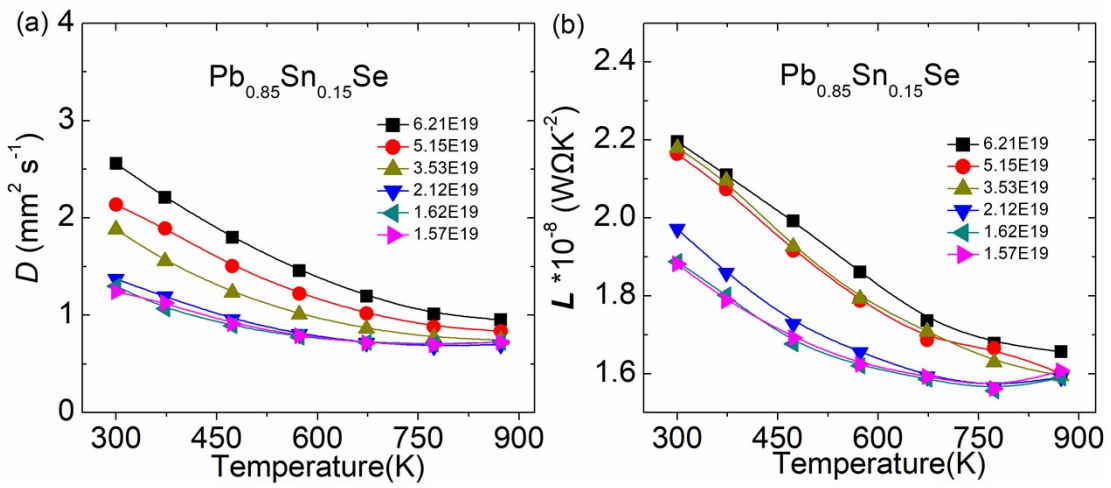

Figure S5. Thermal transport properties of $Pb_{0.85}Sn_{0.15}Se$-based samples: (a) thermal diffusivity and (b) Lorenz number

Table S1. Thermoelectric related parameters of the samples in this work, including sample composition, sample density, carrier density and carrier mobility at room temperature.

Samples	Sample density ($g\ cm^{-3}$)	Carrier density (cm^{-3})	Carrier mobility ($cm^{-2}V^{-1}s^{-1}$)
PbSe	7.93	1.52E20	190
$Pb_{0.95}Sn_{0.05}Se$	7.83	7.89E19	248
$Pb_{0.90}Sn_{0.10}Se$	7.80	7.09E19	230
$Pb_{0.85}Sn_{0.15}Se$	7.62	6.21E19	267
$Pb_{0.80}Sn_{0.20}Se$	7.55	4.80E19	261
$Pb_{0.77}Sn_{0.23}Se$	7.51	3.36E19	236
$Pb_{0.848}Ag_{0.002}Sn_{0.15}Se$	7.65	5.15E19	278
$Pb_{0.847}Ag_{0.003}Sn_{0.15}Se$	7.63	3.53E19	425
$Pb_{0.846}Ag_{0.004}Sn_{0.15}Se$	7.55	2.12E19	473
$Pb_{0.845}Ag_{0.005}Sn_{0.15}Se$	7.54	1.62E19	577
$Pb_{0.844}Ag_{0.006}Sn_{0.15}Se$	7.56	1.57E19	474